JACS
JOURNAL OF THE AMERICAN CHEMICAL SOCIETY
pubs.acs.org/JACS
Article

# Simultaneous Generation of a [2 × 2] Grid-Like Complex and a Linear Double Helicate: a Three-Level Self-Sorting Process

Jean-François Ayme, Jean-Marie Lehn,* Corinne Bailly, and Lydia Karmazin

Cite This: https://dx.doi.org/10.1021/jacs.0c00896
Read Online
ACCESS | Metrics & More | Article Recommendations | Supporting Information

**ABSTRACT:** Two constitutional dynamic libraries (CDLs)—each containing two amines, two dialdehydes, and two metal salts—have been found to self-sort, generating two pairs of imine-based metallosupramolecular architectures (sharing no component) each with a [2 × 2] grid-like complex and a linear double helicate. These CDLs provided unique examples of a three-level self-sorting process, as only two imine-based ligand constituents, two metal complexes, and two architectures were selected during their assembly out of all the possible combinations of their initial components. The metallosupramolecular architectures assembled were characterized by NMR, mass spectroscopy, and X-ray crystallography.

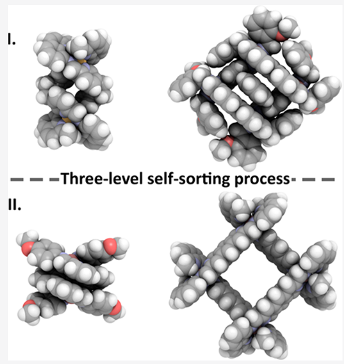




## ■ INTRODUCTION

By addressing both molecular and supramolecular levels, constitutional dynamic chemistry (CDC) has provided chemists with a powerful tool for controlling the organization of chemical systems,[1−3] in particular through the operation of orthogonal self-assembly[4] and self-sorting.[5−9] Illustrative examples of the organizational power of constitutional dynamic systems at both levels can be found in architectures assembled via the condensation of amine and 2-formylpyridine components into dynamic imine-based ligand constituents around transition metal cations.[3a,b,9f−h,10,11]

The concurrent assembly of several of these architectures within the same reaction mixture was shown to promote the emergence of new properties going beyond those of each individual architecture, highlighting the importance of fostering compositional diversity within constitutional dynamic systems in order to extend the scope of their accessible properties.[1c,3b,8a,9f−h,11a−d,h] However, to our knowledge, literature reports only describe the self-assembly of constitutional dynamic architectures having at least one component in common (i.e., organic components and/or type of metal cations).[5,8,9] To increase the compositional diversity of the manifold of assembled architectures, strategies are required that allow the simultaneous control of the outcome of two (or more) interconnected dynamic processes. Such a strategy is offered, namely, by combining imine-based dynamic ligands and by dynamic metal−ligand coordination bond formation.

In the present report, we describe two constitutional dynamic libraries each enabling the concomitant generation of a pair of imine-based metallosupramolecular architectures (sharing no component) each with a [2 × 2] grid-like complex and a linear double helicate, via the self-sorting of their initial six different building blocks. The study provides a unique example of a three-level self-sorting process: (i) at the molecular level, only two specific imine based ligands were formed via the self-sorting of the initial four different amine and aldehyde components; (ii) at the supramolecular level, only two specific metal complexes were generated via the self-sorting of the imine-based ligands around the two types of metal cations used; (iii) finally, only two specific architectures were produced via the self-sorting of the assembled metal complexes.

## ■ RESULTS AND DISCUSSION

1. In the first study, we envisaged that the ligand selectivity of Fe(II) cations should drive the evolution of a mixture of components **1**, **2**, **3**, and **4** toward the exclusive formation of the linear double helicate $[Fe_2(\mathbf{3},\mathbf{4}_2)_2]^{4+}$ and the [2 × 2] grid-like complex $[Cu_4(\mathbf{1},\mathbf{2}_2)_4]^{4+}$ upon addition of Fe(II) and Cu(I) salts (Scheme 1 and Figure 1), the notation $(\mathbf{n},\mathbf{m}_2)$ refers to the imine-based constituent generated by the condensation of aldehyde **n** with two amines **m**. On the basis of previous work from our group[12] and on the preferred octahedral coordination geometry of Fe(II), it was expected that

**Received:** January 23, 2020

**Scheme 1. Structures of Constituents $(\mathbf{1},\mathbf{2}_2)$ and $(\mathbf{3},\mathbf{4}_2)$ Generated by Metallo-Selection during the Self-Sorting of Components 1, 2, 3, and 4 in the Presence of Cu(I) and Fe(II) Salts**

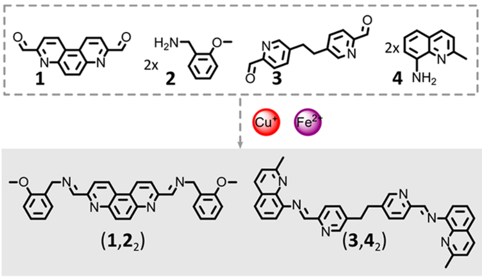

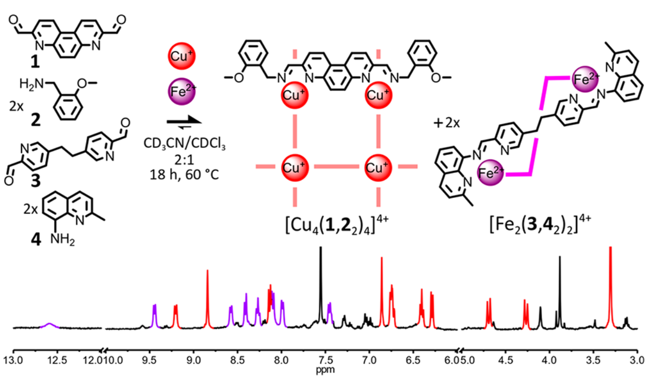

**Figure 1.** Top: Synthesis of complexes $[Cu_4(\mathbf{1},\mathbf{2}_2)_4]^{4+}$ and $[Fe_2(\mathbf{3},\mathbf{4}_2)_2]^{4+}$ through the self-sorting of their initial reactants. Reaction conditions: **1**:**2**:**3**:**4**:$Cu(BF_4)$:$Fe(BF_4)_2$ (1:2:1:2:1:1), $CD_3CN/CDCl_3$ 2:1, 60 °C, 18 h. Bottom: Partial $^1H$ NMR spectrum (400 MHz, $CD_3CN/CDCl_3$ 2:1, 298 K) of the crude reaction mixture after 18 h at 60 °C. The diagnostic signals of the complexes are color coded, $[Cu_4(\mathbf{1},\mathbf{2}_2)_4]^{4+}$ in red and $[Fe_2(\mathbf{3},\mathbf{4}_2)_2]^{4+}$ in purple.

Fe(II) would preferentially bind the least sterically hindered NNN-tridentate ligand accessible from the initial components, namely, the condensation product of **3** with two amines **4**. Subsequent to the formation of $[Fe_2(\mathbf{3},\mathbf{4}_2)_2]^{4+}$, Cu(I) would, by default, have to bind to the moderately sterically hindered bidentate coordination site offered by the condensation product of **1** with two amines **2**. The suitable flexibility of the $CH_2CH_2$ bridge of **3** should ensure that $[Fe_2(\mathbf{3},\mathbf{4}_2)_2]^{4+}$ adopts a linear double helicate architecture,[13,14] while the rigidity and linearity of bis-imine $(\mathbf{1},\mathbf{2}_2)$ and the preferred tetrahedral coordination geometry of Cu(I) should enforce a [2 × 2] grid-like architecture to the $[Cu_4(\mathbf{1},\mathbf{2}_2)_4]^{4+}$ complex.[15,16] Considering the limited steric congestion of **1**, the sterically more demanding 8-amino-2-methylquinoline **4** was preferred over an unsubstituted 8-aminoquinoline to prevent the incorporation of **1** into Fe(II) complexes at equilibrium and to improve the efficiency of the self-sorting process.[12]

2. In a second study, we envisaged that the role of the octahedrally and tetrahedrally coordinated metal cations could be reversed so that, upon the addition of Zn(II) and Cu(I) salts to a mixture of components **4**, **5**, **6**, and **7**, Zn(II) cations would drive the exclusive formation of the [2 × 2] grid-like complex $[Zn_4(\mathbf{5},\mathbf{4}_2)_4]^{8+}$ and, as a corollary, of the linear double helicate $[Cu_2(\mathbf{7},\mathbf{6}_2)_2]^{2+}$ (Scheme 2 and Figure 2). In comparison to Fe(II),

**Scheme 2. Structures of Constituents $(\mathbf{5},\mathbf{4}_2)$ and $(\mathbf{7},\mathbf{6}_2)$ Generated by Metallo-Selection during the Self-Sorting of Components 4, 5, 6, and 7 in the Presence of Cu(I) and Zn(II) Salts**

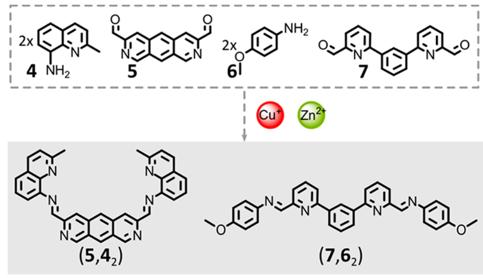

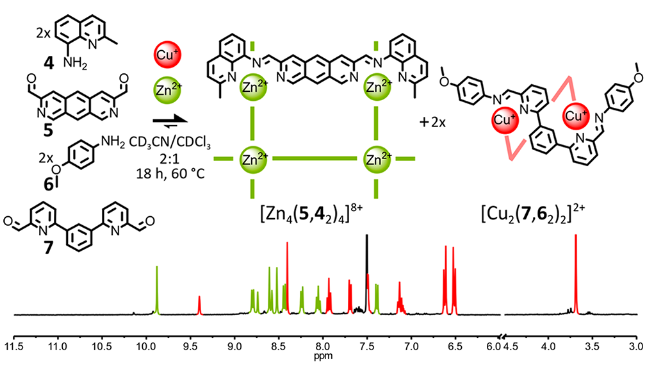

**Figure 2.** Top: Synthesis of complexes $[Cu_2(\mathbf{7},\mathbf{6}_2)_2]^{2+}$ and $[Zn_4(\mathbf{5},\mathbf{4}_2)_4]^{8+}$ through the self-sorting of their initial reactants. Reaction conditions: **4**:**5**:**6**:**7**:$Cu(BF_4)$:$Zn(BF_4)_2$ (2:1:2:1:1:1), $CD_3CN/CDCl_3$ 2:1, 60 °C, 18 h. Bottom: Partial $^1H$ NMR spectrum (400 MHz, $CD_3CN/CDCl_3$ 2:1, 298 K) of the crude reaction mixture after 18 h at 60 °C. The diagnostic signals of the complexes are color coded, $[Cu_2(\mathbf{7},\mathbf{6}_2)_2]^{2+}$ in red and $[Zn_4(\mathbf{5},\mathbf{4}_2)_4]^{8+}$ in green.

Zn(II) cations were shown to require more steric information in their initial set of components to yield a similar degree of self-sorting.[12] Therefore, despite the significant steric congestion provided by the $C_6H_6$ bridge of **7**, the substituted 8-amino-2-methylquinoline **4** was preferred over a regular 8-aminoquinoline to avoid any scrambling of the ligands between the two architectures at equilibrium. The linearity and rigidity of **5** and the coordination preferences of Zn(II) should ensure that $[Zn_4(\mathbf{5},\mathbf{4}_2)_4]^{8+}$ adopts a [2 × 2] grid-like architecture,[15] while the $C_6H_6$ bridge of **7** should allow the twisting of the dinuclear complex $[Cu_2(\mathbf{7},\mathbf{6}_2)_2]^{2+}$ into the helical shape characteristic of a linear double helicate architecture.[13,14]

Before the self-sorting experiments were attempted, the four complexes were prepared separately to confirm their architectures. Each of them was obtained by mixing 1 equiv of the corresponding bis-aldehyde with 2 equiv of the appropriate amine and 1 equiv of the corresponding metal salt in a 2:1 $CD_3CN/CDCl_3$ mixed solvent. The reaction mixtures were analyzed by NMR spectroscopy and ESI-MS after 18 h of heating at 60 °C. As expected for the formation of a [2 × 2] grid-like architecture or a linear double helicate architecture, in all four cases, the $^1H$ NMR spectra of the solutions revealed the formation of highly symmetrical complexes, as all the protons of the ligands of each complex experienced a single chemical and magnetic environment


https://dx.doi.org/10.1021/jacs.0c00896
J. Am. Chem. Soc. XXXX, XXX, XXX−XXX

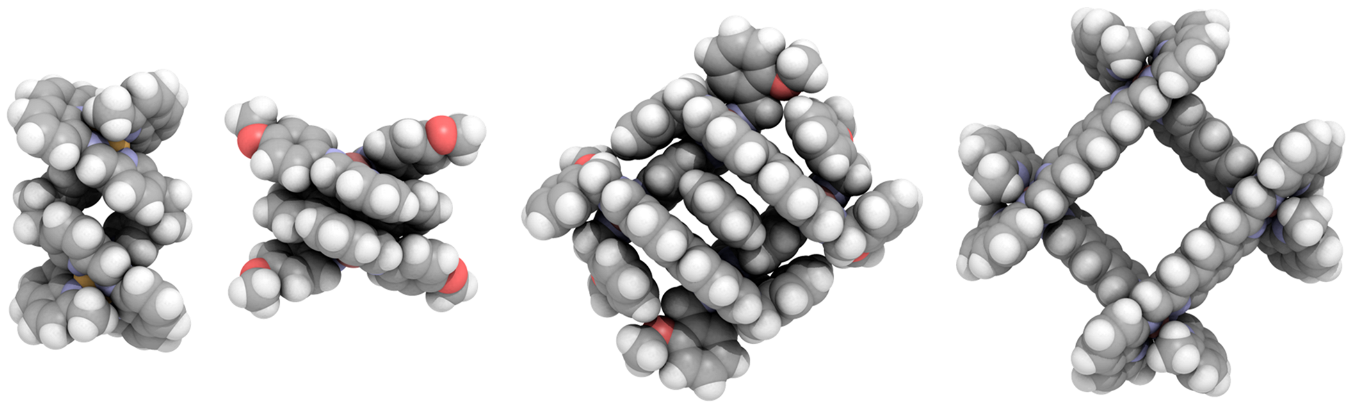

$[Fe_2(\mathbf{3},\mathbf{4}_2)_2](PF_6)_4$ $[Cu_2(\mathbf{7},\mathbf{6}_2)_2](ClO_4)_2$ $[[Cu_4(\mathbf{1},\mathbf{2}_2)_4]\cdot C_6H_6](BPh_4)_4$ $[Zn_4(\mathbf{5},\mathbf{4}_2)_4](BF_4)_8$

**Figure 3.** Single crystal X-ray structures of linear double helicates $[Fe_2(\mathbf{3},\mathbf{4}_2)_2](PF_6)_4$ and $[Cu_2(\mathbf{7},\mathbf{6}_2)_2](ClO_4)_2$ and of [2 × 2] grid-like complexes $[[Cu_4(\mathbf{1},\mathbf{2}_2)_4]\cdot C_6H_6](BPh_4)_4$ and $[Zn_4(\mathbf{5},\mathbf{4}_2)_4](BF_4)_8$. Solvent molecules and counterions have been omitted for clarity.

(Supporting Information, Section 2.2). ESI-MS allowed the determination of the absolute stoichiometry of the metallosupramolecular architectures generated. In each case, $m/z$ fragments matching with the molecular weights of the expected architectures and the loss of $BF_4^-$anions during the ionization process were obtained (Supporting Information, Section 2.2). The analysis of the isotope pattern of these fragments corroborated the formation of the desired complexes. In some cases, additional proof of the nature of the architecture could be obtained. In $^1$H NMR spectroscopy, the N−$CH_2$ protons of $[Cu_4(\mathbf{1},\mathbf{2}_2)_4]^{4+}$ and the $CH_2$ protons of the bridges of $[Fe_2(\mathbf{3},\mathbf{4}_2)_2]^{4+}$ appeared as AB systems ($J$ = 12.8 Hz and $J$ = 11 Hz, respectively). Such AB patterns are characteristic of methylene groups in asymmetric environments, such as the one conferred by the rigid architectures of [2 × 2] grids or linear double helicates.

X-ray-quality crystals of all four architectures were grown by liquid−liquid diffusion (Supporting Information, Section 4). In all cases, subsequent X-ray crystallographic studies established the formation of the desired architecture (Figure 3). The two metal ions of $[Fe_2(\mathbf{3},\mathbf{4}_2)_2](PF_6)_4$ and $[Cu_2(\mathbf{7},\mathbf{6}_2)_2](ClO_4)_2$ are held adjacent by two ligand strands wrapped around each other in a helical fashion. The coordination geometries around both Fe(II) and Cu(I) are distorted octahedra and distorted tetrahedra, respectively. The Cu(I) helicate is more compact than the Fe(II) helicate (Cu,Cu distance is 4.8931(5) Å and Fe,Fe distance is 8.877(2) Å). The metal ions of both $[[Cu_4(\mathbf{1},\mathbf{2}_2)_4]\cdot C_6H_6](BPh_4)_4$ and $[Zn_4(\mathbf{5},\mathbf{4}_2)_4](BF_4)_8$ lie almost in a plane (mean deviation of 0.3665(4) Å and 0.1830 (8) Å, respectively) and form a parallelogram (angles of 79.83 99.17°) and a square (angles of 89.94°), respectively. They display distorted tetrahedral and distorted octahedral coordination of their metal centers to two perpendicularly oriented ligands, respectively. A molecule of benzene lies in the central cavity of the Cu(I) complex (average Cu,Cu distance is 7.913(7) Å) whereas, in the case of the Zn(II) complex, the central cavity is occupied by disordered solvent molecules (average Zn,Zn distance is 11.462(0) Å).

Having shown that all four architectures could be assembled individually, we investigated the formation of $[Cu_4(\mathbf{1},\mathbf{2}_2)_4]^{4+}$ and $[Fe_2(\mathbf{3},\mathbf{4}_2)_2]^{4+}$ on one hand and of $[Cu_2(\mathbf{7},\mathbf{6}_2)_2]^{2+}$ and $[Zn_4(\mathbf{5},\mathbf{4}_2)_4]^{8+}$ on the other hand from mixtures of their initial building blocks. For these two reactions, 1 equiv of each of the metal $BF_4^-$ salts was added to a mixture of 1 equiv of each bis-aldehyde and 2 equiv of each monoamine in a 2:1 $CD_3CN$/$CDCl_3$ mixed solvent. After 18 h of heating at 60 °C, the outcome of both self-assembly processes was analyzed by NMR spectroscopy. In the case of $[Cu_4(\mathbf{1},\mathbf{2}_2)_4]^{4+}$ and $[Fe_2(\mathbf{3},\mathbf{4}_2)_2]^{4+}$(Supporting Information, Figures S30 and S31), the $^1$H NMR spectra of the crude reaction mixture was dominated by the diagnostic signals of the two expected architectures, but some undefined side products were also visible (Figure 1). The limited fidelity of this self-sorting process, especially when compared to the simultaneous generation of related mononuclear complexes,[12] might reflect the need for greater assembly instructions in the initial components to compensate for the increased intricacy of the assembly of polynuclear architectures. In the case of $[Cu_2(\mathbf{7},\mathbf{6}_2)_2]^{2+}$ and $[Zn_4(\mathbf{5},\mathbf{4}_2)_4]^{8+}$ (Supporting Information, Figures S32 and S33), the $^1$H NMR spectrum of the crude reaction mixture revealed the exclusive conversion of the starting materials into a clean mixture of the two metallosupramolecular architectures (Figure 2). The stronger assembly instructions, engraved initially in the components of the system to offset the less defined coordination preferences of Zn(II) compared to Fe(II), were also sufficient to impose the selective assembly of only these two architectures. In both systems, the addition of only one of the two metal cations to the initial library of components did not yield a single complex, exemplifying how the simultaneous assembly of two complexes can operate in synergy and how the higher complexity of a system (i.e., a larger number of components) may result in a simpler output, i.e., "simplexity", as was noted in previous instances.[3b]

## ■ CONCLUSIONS

In the present investigations, we demonstrated that the coordination preferences of tetrahedral and octahedral metal ions can be exploited by ligand design to drive the simultaneous and selective formation of two constitutionally unrelated imine-based metallosupramolecular architectures from their initial reactants. This self-assembly amounts to a three-tier self-sorting process where the organization of the system is controlled at both molecular and supramolecular levels though the correct selection of only two imine-based ligand constituents, two metal complexes, and two architectures from the extended dynamic library of entities potentially accessible via reversible interconnection of the initial reactants.



https://dx.doi.org/10.1021/jacs.0c00896
J. Am. Chem. Soc. XXXX, XXX, XXX−XXX

The present study illustrates the delicate interplay of coordination and structural/conformational features that make up the information characteristics presented by the components and are required for directing the final output of a complex instructed mixture.

Learning how to concurrently control the outcome of multiple dynamic processes shared by several entities within the same reaction mixture is an important step toward increased compositional diversity in constitutional dynamic systems and, ultimately, self-assembling processes that rival biological systems in complexity.

## ■ ASSOCIATED CONTENT

### Supporting Information

The Supporting Information is available free of charge at https://pubs.acs.org/doi/10.1021/jacs.0c00896.

Experimental procedures, spectral data for all compounds, and details of the X-ray analyses (PDF)

Crystallographic data for ($[Cu_2(\mathbf{7},\mathbf{6}_2)_2](ClO_4)_2$·xSolvent) (CIF)

Crystallographic data for ($[Fe_2(\mathbf{3},\mathbf{4}_2)_4](PF_6)_4$·xSolvent) (CIF)

Crystallographic data for ($[[Cu_4(\mathbf{1},\mathbf{2}_2)_4]\cdot C_6H_6](BPh_4)_4$·xSolvent) (CIF)

Crystallographic data for ($[Zn_4(\mathbf{5},\mathbf{4}_2)_4](BF_4)_8$·xSolvent) (CIF)

## ■ AUTHOR INFORMATION

### Corresponding Author

**Jean-Marie Lehn** − *Institute of Nanotechnology, Karlsruhe Institute of Technology, 76344 Eggenstein-Leopoldshafen, Germany; Laboratoire de Chimie Supramoléculaire, Institut de Science et d'Ingénierie Supramoléculaires, Université de Strasbourg, 67000 Strasbourg, France;* orcid.org/0000-0001-8981-4593; Email: lehn@unistra.fr

### Authors

**Jean-François Ayme** − *Institute of Nanotechnology, Karlsruhe Institute of Technology, 76344 Eggenstein-Leopoldshafen, Germany; Laboratoire de Chimie Supramoléculaire, Institut de Science et d'Ingénierie Supramoléculaires, Université de Strasbourg, 67000 Strasbourg, France*

**Corinne Bailly** − *Service de Radiocristallographie, Fédération de chimie Le Bel FR2010, Université de Strasbourg, 67008 Strasbourg, France*

**Lydia Karmazin** − *Service de Radiocristallographie, Fédération de chimie Le Bel FR2010, Université de Strasbourg, 67008 Strasbourg, France*

Complete contact information is available at: https://pubs.acs.org/10.1021/jacs.0c00896

### Funding

The authors acknowledge the financial support by the ERC (Advanced Research Grant SUPRADAPT 290585) and the University of Strasbourg Institute for Advanced Study (USIAS). J.F.A. acknowledges the financial support by the European Union's Horizon 2020 research and innovation program under the Marie Skłodowska-Curie grant agreement No. 749351.

### Notes

The authors declare no competing financial interest.

## ■ ACKNOWLEDGMENTS

J.F.A. gratefully acknowledges Prof. Jack Harrowfield, Dr. Jean-Louis Schmitt, and Cyril Antheaume for extensive discussions.

## ■ ABBREVIATIONS

CDL, constitutional dynamic library; CDC, constitutional dynamic chemistry; NMR, nuclear magnetic resonance; ESI-MS, electrospray ionization mass spectrometry

## ■ REFERENCES

(1) For selected resources on the self-organization of chemical systems: (a) Lehn, J.-M. Perspectives in Chemistry—Steps towards Complex Matter. *Angew. Chem., Int. Ed.* **2013**, *52*, 2836−2850. (b) Ashkenasy, G.; Hermans, T. M.; Otto, S.; Taylor, A. F. Systems Chemistry. *Chem. Soc. Rev.* **2017**, *46*, 2543−2554. (c) Ayme, J.-F.; Lehn, J.-M. From Coordination Chemistry to Adaptive Chemistry. *Adv. Inorg. Chem.* **2018**, *71*, 3−78.

(2) *Constitutional Dynamic Chemistry*; Barboiu, M., Ed.; Topics in Current Chemistry; Springer: Berlin, 2012; Vol. *322*.

(3) For selected recent examples of applications of Constitutional Dynamic Chemistry: (a) Holub, J.; Vantomme, G.; Lehn, J.-M. Training a Constitutional Dynamic Network for Effector Recognition: Storage, Recall, and Erasing of Information. *J. Am. Chem. Soc.* **2016**, *138*, 11783−11791. (b) Men, G.; Lehn, J.-M. Higher Order Constitutional Dynamic Networks: [2 × 3] and [3 × 3] Networks Displaying Multiple, Synergistic and Competitive Hierarchical Adaptation. *J. Am. Chem. Soc.* **2017**, *139*, 2474−2483. (c) Löw, H.; Mena-Osteritz, E.; von Delius, M. Self-Assembled Orthoester Cryptands: Orthoester Scope, Post-Functionalization, Kinetic Locking and Tunable Degradation Kinetics. *Chem. Sci.* **2018**, *9*, 4785−4793. (d) Osypenko, A.; Lehn, J.-M. Pattern Generation and Information Transfer through a Liquid/Liquid Interface in 3D Constitutional Dynamic Networks of Imine Ligands in Response to Metal Cation Effectors. *J. Am. Chem. Soc.* **2019**, *141*, 12724−12737. (e) He, M.; Lehn, J.-M. Time-Dependent Switching of Constitutional Dynamic Libraries and Networks from Kinetic to Thermodynamic Distributions. *J. Am. Chem. Soc.* **2019**, *141*, 18560−18569.

(4) For selected general resources on orthogonal self-assembly: (a) Saha, M. L.; De, S.; Pramanik, S.; Schmittel, M. Orthogonality in Discrete Self-Assembly − Survey of Current Concepts. *Chem. Soc. Rev.* **2013**, *42*, 6860−6909. (b) Wilson, A.; Gasparini, G.; Matile, S. Functional Systems with Orthogonal Dynamic Covalent Bonds. *Chem. Soc. Rev.* **2014**, *43*, 1948−1962. (c) Wei, P.; Yan, X.; Huang, F. Supramolecular Polymers Constructed by Orthogonal Self-Assembly Based on Host−Guest and Metal−Ligand Interactions. *Chem. Soc. Rev.* **2015**, *44*, 815−832.

(5) For selected general resources on self-sorting: (a) Kramer, R.; Lehn, J.-M.; Marquis-Rigault, A. Self-Recognition in Helicate Self-Assembly: Spontaneous Formation of Helical Metal Complexes from Mixtures of Ligands and Metal Ions. *Proc. Natl. Acad. Sci. U. S. A.* **1993**, *90*, 5394−5398. (b) Rowan, S. J.; Hamilton, D. G.; Brady, P. A.; Sanders, J. K. M. Automated Recognition, Sorting, and Covalent Self-Assembly by Predisposed Building Blocks in a Mixture. *J. Am. Chem. Soc.* **1997**, *119*, 2578−2579. (c) Wu, A.; Isaacs, L. Self-Sorting: The Exception or the Rule? *J. Am. Chem. Soc.* **2003**, *125*, 4831−4835. (d) Safont-Sempere, M. M.; Fernández, G.; Würthner, F. Self-Sorting Phenomena in Complex Supramolecular Systems. *Chem. Rev.* **2011**, *111*, 5784−5814. (e) He, Z.; Jiang, W.; Schalley, C. A. Integrative Self-Sorting: a Versatile Strategy for the Construction of Complex Supramolecular Architecture. *Chem. Soc. Rev.* **2015**, *44*, 779−789. (f) Hsu, C.-W.; Miljanić, O. Š. *Dynamic Covalent Chemistry: Principles, Reactions, and Applications*, Zhang, W.; Jin, Y., Eds., John Wiley & Sons Ltd:: Chichester, UK, 2017; pp 253−284;. (g) Schmittel, M.; Saha, S. From Self-Sorting of Dynamic Metal-Ligand Motifs to (Supra)molecular Machinery in Action. *Adv. Inorg. Chem.* **2018**, *71*, 135−176.

(6) For selected examples of self-sorting processes based on dynamic covalent bonds: (a) Içli, B.; Christinat, N.; Tönnemann, J.; Schüttler, C.; Scopelliti, R.; Severin, K. Synthesis of Molecular Nanostructures by Multicomponent Condensation Reactions in a Ball Mill. *J. Am. Chem. Soc.* **2009**, *131*, 3154−3155. (b) Hsu, C. W.; Miljanić, O. Š. Adsorption-Driven Self-Sorting of Dynamic Imine Libraries. *Angew. Chem., Int. Ed.* **2015**, *54*, 2219−2222. (c) Klotzbach, S.; Beuerle, F. Shape-Controlled Synthesis and Self-Sorting of Covalent Organic Cage Compounds. *Angew. Chem., Int. Ed.* **2015**, *54*, 10356−10360.

(7) For selected examples of self-sorting processes based on metal complexes: (a) Zheng, Y. R.; Yang, H. B.; Ghosh, K.; Zhao, L.; Stang, P. J. Multicomponent Supramolecular Systems: Self-Organization in Coordination-Driven Self-Assembly. *Chem. - Eur. J.* **2009**, *15*, 7203−7214. (b) Johnson, A. M.; Hooley, R. J. Steric Effects Control Self-Sorting in Self-Assembled Clusters. *Inorg. Chem.* **2011**, *50*, 4671−4673. (c) Lu, X.; Li, X.; Guo, K.; Xie, T.-Z.; Moorefield, C. N.; Wesdemiotis, C.; Newkome, G. R. Probing a Hidden World of Molecular Self-Assembly: Concentration-Dependent, Three-Dimensional Supramolecular Interconversions. *J. Am. Chem. Soc.* **2014**, *136*, 18149−18155. (d) Bloch, W. M.; Holstein, J. J.; Hiller, W.; Clever, G. H. Morphological Control of Heteroleptic *cis*- and *trans*-$Pd_2L_2L'_2$ Cages. *Angew. Chem., Int. Ed.* **2017**, *56*, 8285−8289.

(8) For selected examples of self-sorting processes based on constitutional dynamic metal complexes: (a) Jiménez, A.; Bilbeisi, R. A.; Ronson, T. K.; Zarra, S.; Woodhead, C.; Nitschke, J. R. Selective Encapsulation and Sequential Release of Guests Within a Self-Sorting Mixture of Three Tetrahedral Cages. *Angew. Chem., Int. Ed.* **2014**, *53*, 4556−4560. (b) Ayme, J.-F.; Beves, J. E.; Campbell, C. J.; Leigh, D. A. The Self-Sorting Behavior of Circular Helicates and Molecular Knots and Links. *Angew. Chem., Int. Ed.* **2014**, *53*, 7823−7827. (c) Holloway, L. R.; Young, M. C.; Beran, G. J.; Hooley, R. J. High Fidelity Sorting of Remarkably Similar Components *via* Metal-Mediated Assembly. *Chem. Sci.* **2015**, *6*, 4801−4806. (d) Johnson, A. M.; Wiley, C. A.; Young, M. C.; Zhang, X.; Lyon, Y.; Julian, R. R.; Hooley, R. J. Narcissistic Self-Sorting in Self-Assembled Cages of Rare Earth Metals and Rigid Ligands. *Angew. Chem., Int. Ed.* **2015**, *54*, 5641−5645. (e) Wiley, C. A.; Holloway, L. R.; Miller, T. F.; Lyon, Y.; Julian, R. R.; Hooley, R. J. Electronic Effects on Narcissistic Self-Sorting in Multicomponent Self-Assembly of Fe-Iminopyridine *meso*-Helicates. *Inorg. Chem.* **2016**, *55*, 9805−9815. (f) Holloway, L. R.; Bogie, P. M.; Hooley, R. J. Controlled Self-Sorting in Self-Assembled Cage Complexes. *Dalton Trans.* **2017**, *46*, 14719−14723.

(9) For selected examples on self-sorting processes involving supramolecular architectures built around more than one type of metal template: (a) Sun, X.; Johnson, D. W.; Caulder, D. L.; Powers, R. E.; Raymond, K. N.; Wong, E. H. Exploiting Incommensurate Symmetry Numbers: Rational Design and Assembly of $M_2M'_3$, $L_6$Supramolecular Clusters with $C_{3h}$ Symmetry. *Angew. Chem., Int. Ed.* **1999**, *38*, 1303−1307. (b) Ibukuro, F.; Fujita, M.; Yamagushi, K.; Sauvage, J.-P. Quantitative and Spontaneous Formation of a Doubly Interlocking [2]Catenane Using Copper(I) and Palladium(II) as Templating and Assembling Centers. *J. Am. Chem. Soc.* **1999**, *121*, 11014−11015. (c) Wise, M. D.; Holstein, J. J.; Pattison, P.; Besnard, C.; Solari, E.; Scopelliti, R.; Bricogne, G.; Severin, K. Large, Heterometallic Coordination Cages Based on Ditopic Metallo-Ligands with 3-Pyridyl Donor Groups. *Chem. Sci.* **2015**, *6*, 1004−1010. (d) Sepehrpour, H.; Saha, M. L.; Stang, P. J. Fe−Pt Twisted Heterometallic Bicyclic Supramolecules via Multicomponent Self-Assembly. *J. Am. Chem. Soc.* **2017**, *139*, 2553−2556. (e) Gaikwad, S.; Saha, M. L.; Samanta, D.; Schmittel, M. Five-Component Trigonal Nanoprism with Six Dynamic Corners. *Chem. Commun.* **2017**, *53*, 8034−8037. (f) Saha, M. L.; Schmittel, M. From 3-Fold Completive Self-Sorting of a Nine-Component Library to a Seven-Component Scalene Quadrilateral. *J. Am. Chem. Soc.* **2013**, *135*, 17743−17746. (g) Ramsay, W. J.; Szczypinski, F. T.; Weissman, H.; Ronson, T. K.; Smulders, M. M. J.; Rybtchinski, B.; Nitschke, J. R. Designed Enclosure Enables Guest Binding Within the 4200 $Å^3$ Cavity of a Self-Assembled Cube. *Angew. Chem., Int. Ed.* **2015**, *54*, 5636−5640. (h) Rizzuto, F. J.; Ramsay, W. J.; Nitschke, J. R. Otherwise Unstable Structures Self-Assemble in the Cavities of Cuboctahedral Coordination Cages. *J. Am. Chem. Soc.* **2018**, *140*, 11502−11509.

(10) For selected examples of the diversity of metallo-supramolecular architectures reachable from amine-and 2-formylpyridine-containing components: (a) Chichak, K. S.; Cantrill, S. J.; Pease, A. R.; Chiu, S.-H.; Cave, G. W. V.; Atwood, J. L.; Stoddart, J. F. Molecular Borromean Rings. *Science* **2004**, *304*, 1308−1312. (b) Nitschke, J. R. Construction, Substitution, and Sorting of Metallo-organic Structures via Subcomponent Self-Assembly. *Acc. Chem. Res.* **2007**, *40*, 103−112. (c) Ayme, J.-F.; Beves, J. E.; Leigh, D. A.; McBurney, R. T.; Rissanen, K.; Schultz, D. A Synthetic Molecular Pentafoil Knot. *Nat. Chem.* **2012**, *4*, 15−20. (d) Beves, J. E.; Campbell, C. J.; Leigh, D. A.; Pritchard, R. G. Tetrameric Cyclic Double Helicates as a Scaffold for a Molecular Solomon Link. *Angew. Chem., Int. Ed.* **2013**, *52*, 6464−6467. (e) Wood, C. S.; Ronson, T. K.; Belenguer, A. M.; Holstein, J. J.; Nitschke, J. R. Two-Stage Directed Self-Assembly of a Cyclic [3]catenane. *Nat. Chem.* **2015**, *7*, 354−358.

(11) For selected examples of the functional potential of metallosupramolecular architecture built from amine-and 2-formylpyridine-containing components: *Potential for adaptation to stimuli*, see ref 2. and (a) Campbell, V. E.; de Hatten, X.; Delsuc, N.; Kauffmann, B.; Huc, I.; Nitschke, J. R. Cascading Transformations within a Dynamic Self-Assembled System. *Nat. Chem.* **2010**, *2*, 684−687. (b) McConnell, A. J.; Wood, C. S.; Neelakandan, P. P.; Nitschke, J. R. Stimuli-Responsive Metal−Ligand Assemblies. *Chem. Rev.* **2015**, *115*, 7729−7793. (c) Roberts, D. A.; Pilgrim, B. S.; Nitschke, J. R. Covalent Post-Assembly Modification in Metallosupramolecular Chemistry. *Chem. Soc. Rev.* **2018**, *47*, 626−644. (d) Roberts, D. A.; Pilgrim, B. S.; Sirvinskaite, G.; Ronson, T. K.; Nitschke, J. R. Covalent Post-assembly Modification Triggers Multiple Structural Transformations of a Tetrazine-Edged Fe4L6 Tetrahedron. *J. Am. Chem. Soc.* **2018**, *140*, 9616−9623. (e) Pramanik, S.; Aprahamian, I. Hydrazone Switch-Based Negative Feedback Loop. *J. Am. Chem. Soc.* **2016**, *138*, 15142−15145. *Potential as molecular container* (f) Zarra, S.; Wood, D. M.; Roberts, D. A.; Nitschke, J. R. Molecular Containers in Complex Chemical Systems. *Chem. Soc. Rev.* **2015**, *44*, 419−432. *Potential as biologically active molecules or as mimic of biological molecules* (g) Kaner, R.; Allison, S.; Faulkner, A.; Phillips, R.; Roper, D.; Shepherd, S.; Simpson, D.; Waterfield, N.; Scott, P. Anticancer Metallohelices: Nanomolar Potency and High Selectivity. *Chem. Sci.* **2016**, *7*, 951−958. *Potential in polymeric materials* (h) Chow, C.-F.; Fujii, S.; Lehn, J.-M. Metallodynamers: Neutral Double-Dynamic Metallosupramolecular Polymers. *Chem. - Asian J.* **2008**, *3*, 1324−1335. (i) Ulrich, S.; Lehn, J.-M. Reversible Switching between Macrocyclic and Polymeric States by Morphological Control in a Constitutional Dynamic System. *Angew. Chem., Int. Ed.* **2008**, *47*, 2240−2243. *Potential as anion binder* (j) Ayme, J.-F.; Beves, J. E.; Campbell, C. J.; Gil-Ramírez, G.; Leigh, D. A.; Stephens, A. J. Strong and Selective Anion Binding within the Central Cavity of Molecular Knots and Links. *J. Am. Chem. Soc.* **2015**, *137*, 9812−9815. (k) Bilbeisi, R. A.; Prakasam, T.; Lusi, M.; El-Khoury, R.; Platas-Iglesias, C.; Charbonnière, L. J.; Olsen, J.-C.; Elhabiri, M.; Trabolsi, A. [C−H···Anion] Interactions Mediate the Templation and Anion Binding Properties of Topologically Non-Trivial Metal−Organic Structures in Aqueous Solutions. *Chem. Sci.* **2016**, *7*, 2524−2532.

(12) Ayme, J.-F.; Lehn, J.-M. Self-Sorting of Two Imine-Based Metal Complexes: Balancing Kinetics and Thermodynamics in Constitutional Dynamic Networks. *Chem. Sci.* **2020**, *11*, 1114−1121.

(13) For selected examples on metallo−supramolecular helicates: (a) Constable, E. C. *Comprehensive Supramolecular Chemistry*; Atwood, J. L., Davies, J. E. D., Macnicol, D. D., Vögtle, F., Lehn, J.-M., Eds.; Pergamon: Oxford, 1996; Vol. 9; pp 213−252;. (b) Piguet, C.; Bernardinelli, G.; Hopfgartner, G. Helicates as Versatile Supramolecular Complexes. *Chem. Rev.* **1997**, *97*, 2005−2062. (c) Yashima, E.; Ousaka, N.; Taura, D.; Shimomura, K.; Ikai, T.; Maeda, K. Supramolecular Helical Systems: Helical Assemblies of Small Molecules, Foldamers, and Polymers with Chiral Amplification and Their Functions. *Chem. Rev.* **2016**, *116*, 13752−13990.


https://dx.doi.org/10.1021/jacs.0c00896
J. Am. Chem. Soc. XXXX, XXX, XXX−XXX

(14) Rapenne, G.; Dietrich-Buchecker, C.; Sauvage, J.-P. Copper(I)- or Iron(II)-Templated Synthesis of Molecular Knots Containing Two Tetrahedral or Octahedral Coordination Sites. *J. Am. Chem. Soc.* **1999**, *121*, 994−1001.

(15) For selected examples on [2 × 2] grid-like complexes: (a) Ruben, M.; Rojo, J.; Romero-Salguero, F. J.; Uppadine, L. H.; Lehn, J.-M. Grid-Type Metal Ion Architectures: Functional Metallosupramolecular Arrays. *Angew. Chem., Int. Ed.* **2004**, *43*, 3644−3662. (b) Dawe, L. N.; Shuvaev, K. V.; Thompson, L. K. Polytopic Ligand Directed Self-Assembly—Polymetallic [$n \times n$] Grids versus Non-Grid Oligomers. *Chem. Soc. Rev.* **2009**, *38*, 2334−2359. (c) Hardy, J. G. Metallosupramolecular Grid Complexes: towards Nanostructured Materials with High-Tech Applications. *Chem. Soc. Rev.* **2013**, *42*, 7881−7899.

(16) Baxter, P. N. W.; Lehn, J.-M.; Kneisel, B. O.; Fenske, D. Self-Assembly of a Symmetric Tetracopper Box-Grid with Guest Trapping in the Solid State. *Chem. Commun.* **1997**, 2231−2232.



https://dx.doi.org/10.1021/jacs.0c00896
*J. Am. Chem. Soc.* XXXX, XXX, XXX−XXX